JOURNAL OF MATERIALS SCIENCE 32 (1997) 497–502

Synthesis and characterization of molybdenum disulphide formed from ammonium tetrathiomolybdate

H.W. WANG, P. SKELDON, G.E. THOMPSON, G.C. WOOD
Corrosion and Protection Centre, University of Manchester Institute of Science and Technology, PO Box 88, Manchester M60 1QD, UK

An investigation has been carried out into the possibility of *in situ* formation of MoS_2 within porous anodic films on aluminium, to improve subsequent tribological behaviour, by re-anodizing in thiomolybdate electrolyte. Acidification of thiomolybdate was employed to simulate the conditions for formation of the sulphide at the anodic film/electrolyte interface, followed by appropriate vacuum heat treatments to study possible temperature effects on the sulphide due to either friction or Joule heating during anodizing. The products of both acidification and heat treatment, characterized by X-ray powder diffraction and scanning electron microscopy, were compared with those formed by direct thermal decomposition of ammonium tetrathiomolybdate crystals. The precipitate formed by acidification was mainly amorphous molybdenum trisulphide (MoS_3), which on heat treatment at 450 and 850 °C yielded 3R-MoS_2. 3R-MoS_2 also formed by the thermal decomposition of thiomolybdate crystals. Thermogravimetric and differential thermal analyses showed that the decomposition of MoS_3 to MoS_2 occurred in the range 220–370 °C and revealed the sequence of reaction steps. The findings suggest that mainly amorphous MoS_3 is formed as a consequence of changes in the pH of the film/electrolyte interface during re-anodizing but the product is relatively easily transformed to crystalline MoS_2 on moderate heating which may occur during wear processes.

1. Introduction

Molybdenum disulphide has been the subject of significant research for applications including non-aqueous lithium batteries [1], catalytic hydrodesulphurization of petroleum [2], and wear resistance [3–5]. With regard to the last of these, its successful application originates largely from easy cleavage of crystalline MoS_2 in the [0 0 1] direction along which (S–Mo–S) layers are stacked [6]. Apart from its natural form, MoS_2 can be synthesized by high-temperature solid state reaction between molybdenum and sulphur powders in vacuum [7–9], thermal decomposition of ammonium tetrathiomolybdate [10, 11] or amorphous molybdenum trisulphide [9, 12], thermally assisted transition of amorphous MoS_2 powders [13] and other techniques, such as sputtering [14], electrodeposition [15] and chemical deposition [16]. For tribological applications involving aluminium, recent research has been directed to incorporating molybdenum sulphide into porous anodic films on aluminium, during re-anodizing in thiomolybdate electrolyte [17, 18]. The sulphide, the precise composition of which is unknown, is formed *in situ* within the pores, as distinct from incorporation of MoS_2 formed *ex situ* [19].

The main anodic reaction during re-anodizing of aluminium, with a pre-formed porous film, in thiomolybdate electrolyte results in proton generation at the pore base/electrolyte interface as follows:

$$2Al + 3H_2O = Al_2O_3 + 6H^+ + 6e \quad (1)$$

The pH reduction, stemming from the generation of H^+ cations at the pore bases, and subsequent reaction with thiomolybdate anions lead to *in situ* formation of the sulphide precipitate. In view of the relatively numerous types of molybdenum sulphide, including amorphous molybdenum trisulphide [11, 12], disulphide, (both rhombohedral and hexagonal polytypes) [11, 20–25], sesquisulphide [26], and others such as Mo_3S_4 [27], $Mo_{15}S_{19}$ [28], and Mo_2S_5 [29], further study of the sulphide precipitate is required. In the present work the probable composition and structure of the sulphide produced during anodizing, and also the influence of heating of the sulphide, which may occur during wear processes, is determined. An acidification procedure, which simulates anodizing conditions at the film/electrolyte interface, is employed to form sufficient precipitate for analyses. The influence of the electric field at the film/electrolyte interface during anodizing is not considered important to the development of the sulphide since the precipitate forms above the anodic film outside the region of high field.

0022–2461 © *1997 Chapman & Hall*

2. Experimental details

2.1. Acidification procedure

A 10^{-2} M solution of ammonium tetrathiomolybdate (purity 99.97% (Aldrich Chemicals)) was acidified by addition of dilute H_2SO_4 (5%), causing the initially dark brown solution to form black precipitates, which deposited when stirring was stopped. Upon removing the colourless solution, the black residue was washed thoroughly in acetone, collected by filtration, washed again in ethanol, dried at about 80 °C for 10 min, and finally kept in the laboratory environment for 24 h prior to examination.

2.2. Precipitate heat treatment and examination

The precipitates were characterized using X-ray diffraction (XRD) and scanning electron microscopy (SEM) before and after vacuum heat treatments (10^{-6} torr (1 torr = 133.3 Pa)) at 450 °C for 2 h and at 850 °C for 5 h (furnace-cooled). For comparison, ammonium tetrathiomolybdate crystals were thermally decomposed in vacuum and also examined by simultaneous thermogravimetric analysis and differential thermal analysis (TGA/DTA) using an argon atmosphere and a temperature ramp of 10 °C min^{-1}. The reference material was alumina. The mass loss ratio (ΔW), and temperature difference (ΔT) of the samples were recorded.

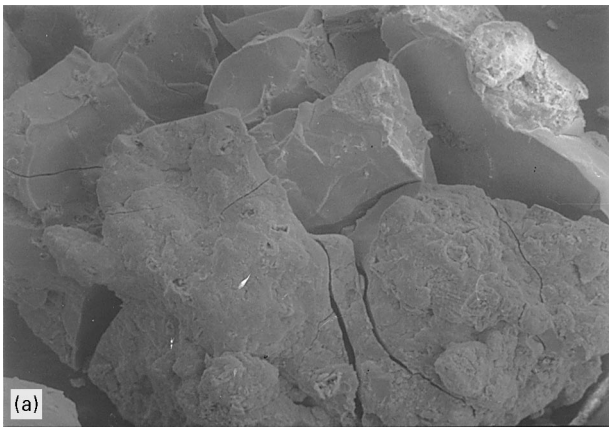

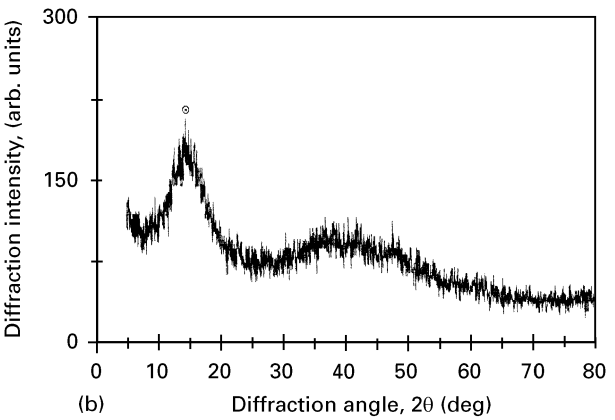

Figure 1 (a) Morphology and (b) the X-ray diffraction pattern of the precipitates (amorphous molysulphide) formed by adding of 50 ml of dilute H_2SO_4 (5%) to 1000 ml of 10^{-2} M $(NH_4)_2MoS_4$ solution.

3. Results, discussion and conclusions

3.1. As-formed precipitate

Fig. 1a shows a scanning electron micrograph of the dull-grey product of acidifying the thiomolybdate solution, which reveals irregularly-shaped agglomerates. X-ray diffraction of the pulverized precipitates gave a broad peak at $2\theta = 14.2°$ and a very diffuse peak at $2\theta = 35$–$45°$ (Fig. 1b), with the latter indicating that the precipitates were mainly amorphous. A small amount of crystalline material is present, identified from the peak at $2\theta = 14.2°$, which is the first strongest peak ($I = 100\%$) for 3R-MoS_2 [21, 30]. The following chemical reaction is suggested to proceed during acidification:

$$MoS_4^{2-} + 2H^+ \rightarrow MoS_3\downarrow + H_2S\uparrow \qquad (2)$$

Only the amorphous state has been reported for MoS_3 [12, 31], whereas MoS_2 can occasionally be amorphous [12]. In view of the latter observation, although considered less likely, the precipitates could also be amorphous MoS_2 and sulphur, if the following reaction involving reduction of molybdenum species occurred:

$$MoS_4^{2-} + 2H^+ = MoS_2\downarrow + H_2S\uparrow + S\downarrow \qquad (3)$$

The trace amount of MoS_2 crystals, indicated by X-ray diffraction, may have formed from direct precipitation from the solution, crystallization of amorphous MoS_2, or decomposition of amorphous MoS_3 which loses sulphur [12] and is transformed to crystalline MoS_2.

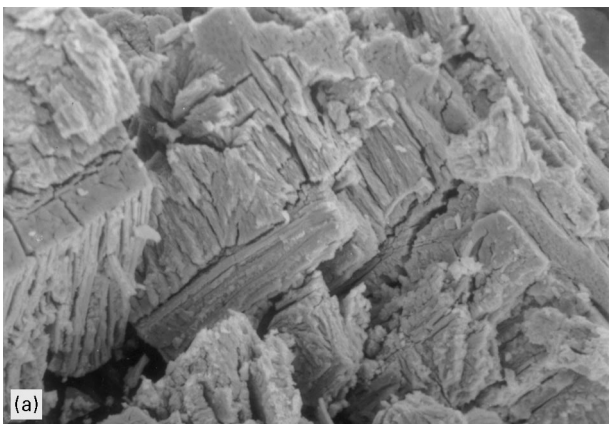

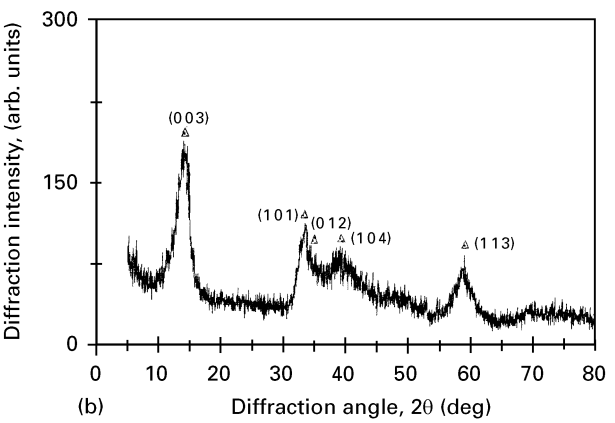

Figure 2 (a) Morphology and (b) the X-ray diffraction pattern of the precipitates (3R-MoS_2), formed under conditions of Fig. 1, after heat treatment at 450 °C for 2 h at 10^{-6} torr.

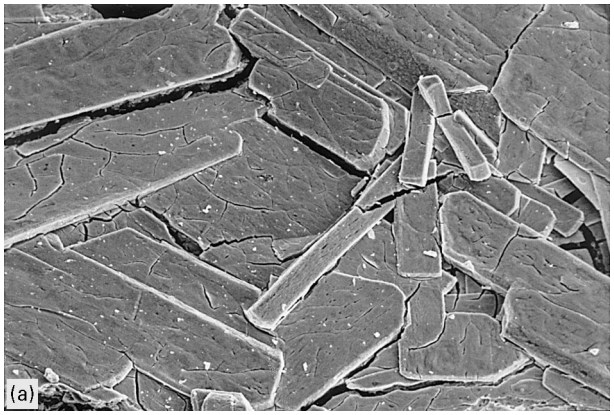

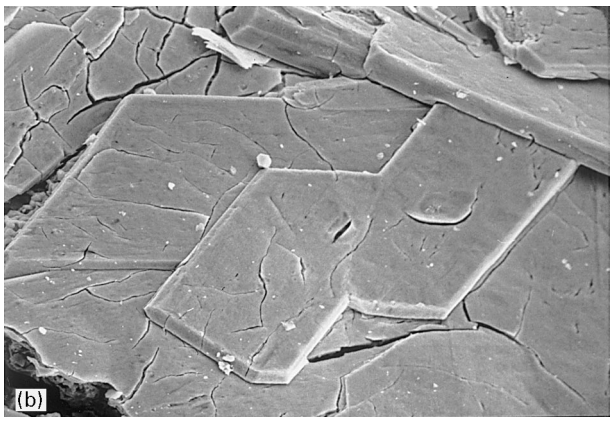

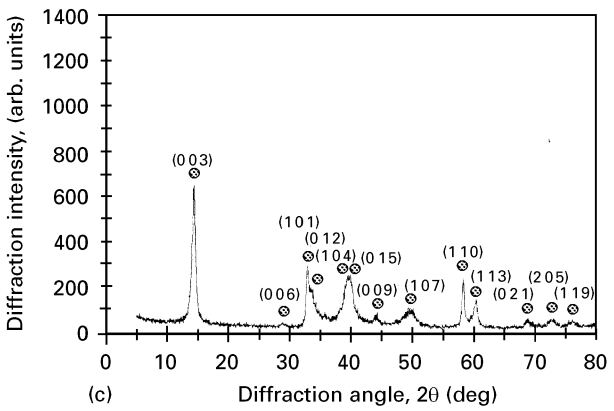

Figure 3 (a) and (b) Morphology and (c) the X-ray diffraction pattern of the precipitates (◎-3R-MoS_2), formed under conditions of Fig. 1, after heat treatment at 850 °C for 5 h at 10^{-6} torr.

3.2. Effect of vacuum heat treatment

The initial precipitates were markedly different in appearance from the grey, shiny crystalline flakes, of laminar appearance, formed after heat treatment at 450 °C (Fig. 2a). X-ray diffraction of the pulverized material reveals five relatively sharp peaks, arising from 3R-MoS_2 (Fig. 2b), which is considered to be formed by the dissociation of MoS_3.

$$MoS_3 = MoS_2 + S\uparrow \quad (4)$$

Heat treatment at increased temperature for prolonged times (850 °C for 5 h) allowed more extensive growth of the crystalline product than at lower temperature. Fig. 3a and b shows the well-crystallized, layered product and cleaved crystals. X-ray diffraction of the pulverized crystals, disclosed additional peaks to the five of Fig. 2b, which are now sharper and of increased intensity (Fig. 3c); the peaks have been indexed giving good agreement with those of 3R-MoS_2 [21, 30].

The synthesis of crystalline MoS_2, from the acidification and heat treatment procedure, has been accompanied by study of the thermal decomposition of ammonium tetrathiomolybdate crystals. The crystals, with the XRD pattern of Fig. 4a, developed 3R-MoS_2 after heat treatment at 450 or 850 °C, similar to that produced by heat treatment of the as-formed precipitate (Fig. 4b–f). For ready comparison of the products relevant data are drawn together in Fig. 5.

3.3. TGA/DTA

It is of practical value to determine the transition temperature ranges for the formation of products of heat-treated MoS_3. Thermal decomposition of thiomolybdate is an established method for preparing MoS_3 [12, 32]. Fig. 6 shows the resultant TGA/DTA profiles. From the TGA curve, five decomposition reactions are identified, with mass loss ratios of 2.2, 33.2, 5.1, 10.7 and 5.5%, respectively. Five peaks are revealed on the corresponding DTA curve, the first two endothermic, the third and fourth exothermic, and the last endothermic. The first decomposition, in the range 50–160 °C arises from dehydration of the starting material which caused 2.2% mass loss. The second in the range 160–270 °C, causing an accumulated mass loss of 35.4% (2.2% + 33.2%), suggests formation of Mo_2S_5, which results in a calculated 34.4% mass difference by the reaction. To the authors' knowledge there has been no convincing report of the existence of Mo_2S_5; thus a mixture of MoS_3/MoS_2, in a ratio of 1:1, was probably formed by the reaction:

$$2(NH_4)_2MoS_4 = MoS_3 + MoS_2 + 2H_2S\uparrow + 4NH_3\uparrow + S\uparrow \text{ (Endothermic, 160–270 °C)} \quad (5)$$

The third decomposition (270–370 °C), leading to a total mass loss ratio of 40.5% (2.2% + 33.2% + 5.1%), suggests formation of MoS_2 (calculated mass loss 40.3%) by the reaction:

$$MoS_3 = MoS_2 + S\uparrow \text{(Endothermic, 270–370 °C)} \quad (6)$$

The DTA curve in this temperature range revealed an exothermic peak, which probably originated from the amorphous–crystalline transition of MoS_2 according to the reaction:

$$MoS_2 \text{ (Amorphous)} = MoS_2 \text{ (Rhombohedral polytype) (Exothermic)} \quad (7)$$

An overall heat generation for Reactions 6 and 7 was evident which, although there is a lack of relevant thermal property data, is believed to stem from both the heat released during the amorphous–crystalline transition, and the thermal property difference between MoS_3 and MoS_2.

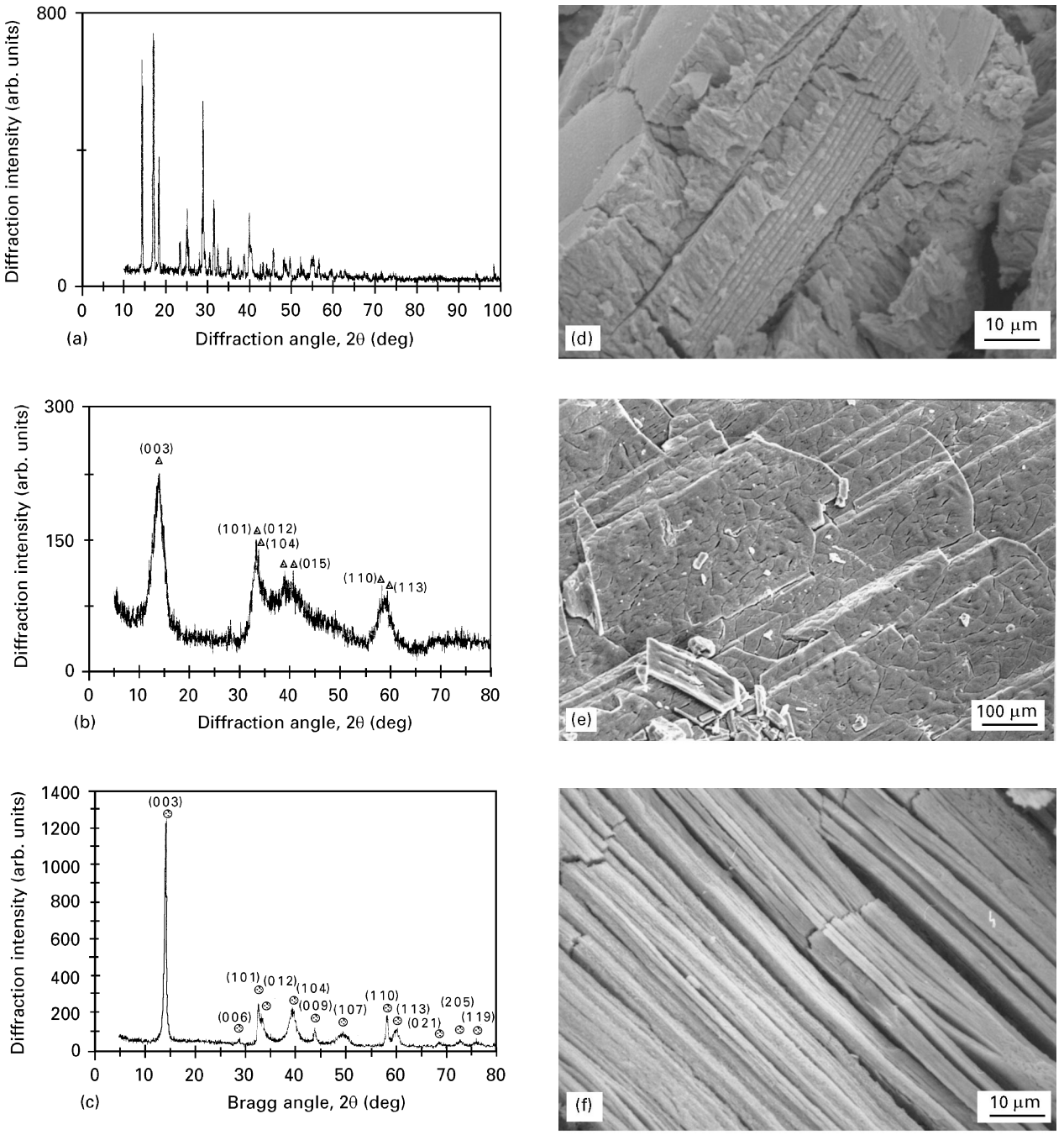

Figure 4 X-ray diffraction patterns and morphologies of the products, formed by the decomposition of $(NH_4)_2MoS_4$ crystals of diffraction patterns shown in (a), after heat treatment in a vacuum of 10^{-6} torr at (b) and (d) 450 °C, 2h, (c), (e) and (f) 850 °C, 5 h ((b) ▲--- 3R-MoS_2 and (c) ⊗--- 3R-MoS_2).

At still higher temperature the effect of residual oxygen contamination in the argon was detected. Between 370–700 °C, two exothermic reactions led to total accumulated mass loss ratios of 51.2 and 56.7%, which are consistent with the ratios for MoO_2 (52.3%) and Mo_2O_3 (55.3%), respectively, produced by the reactions:

$$MoS_2 + O_2 = MoO_2 + 2S\uparrow \quad \text{(Exothermic, 370–430 °C)} \quad (8)$$

$$4MoO_2 = 2Mo_2O_3 + O_2\uparrow \quad \text{(Exothermic, 440–550 °C)} \quad (9)$$

Because of the rapid decomposition of MoS_3 within a narrow temperature range, the TGA/DTA curves failed to reveal a clear temperature range for the formation of MoS_3. From the TGA curve, the formation of MoS_3 from thiomolybdate crystals occurs at temperatures as low as 160 °C and is completed at 270 °C. Previous studies of the decomposition showed that MoS_3 lost sulphur when heated above 250 °C [12, 32], but the product remained amorphous up to approximately 350 °C [12]. These results are in fair agreement with the present findings, particularly when factors influencing the TGA/DTA curves, including both instrumental factors (heating rate, furnace atmosphere, sample holder, etc.) and material factors (sample mass, particle size, thermal property, etc.), are considered [33]. Indeed, the formation of MoS_3 by decomposition of $(NH_4)_2MoS_4$ and the formation of

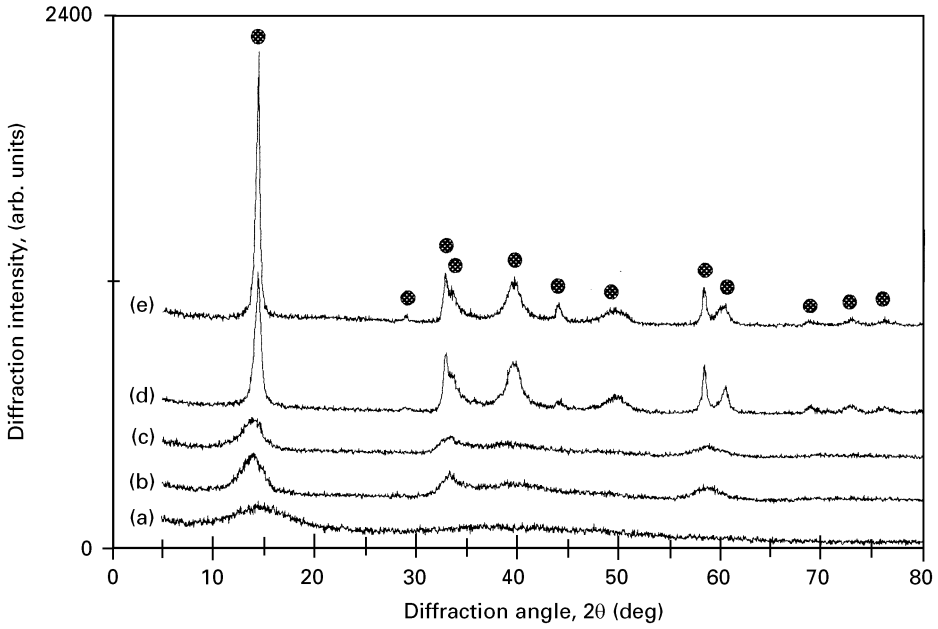

Figure 5 Comparison of X-ray diffraction patterns of products shown in Figs 1–4 ((a), (c), and (d) concern the product formed by acidification and its transition, (b) and (e) concern the product formed by decomposition of ATT. ⊗ - - - 3R-MoS_2).

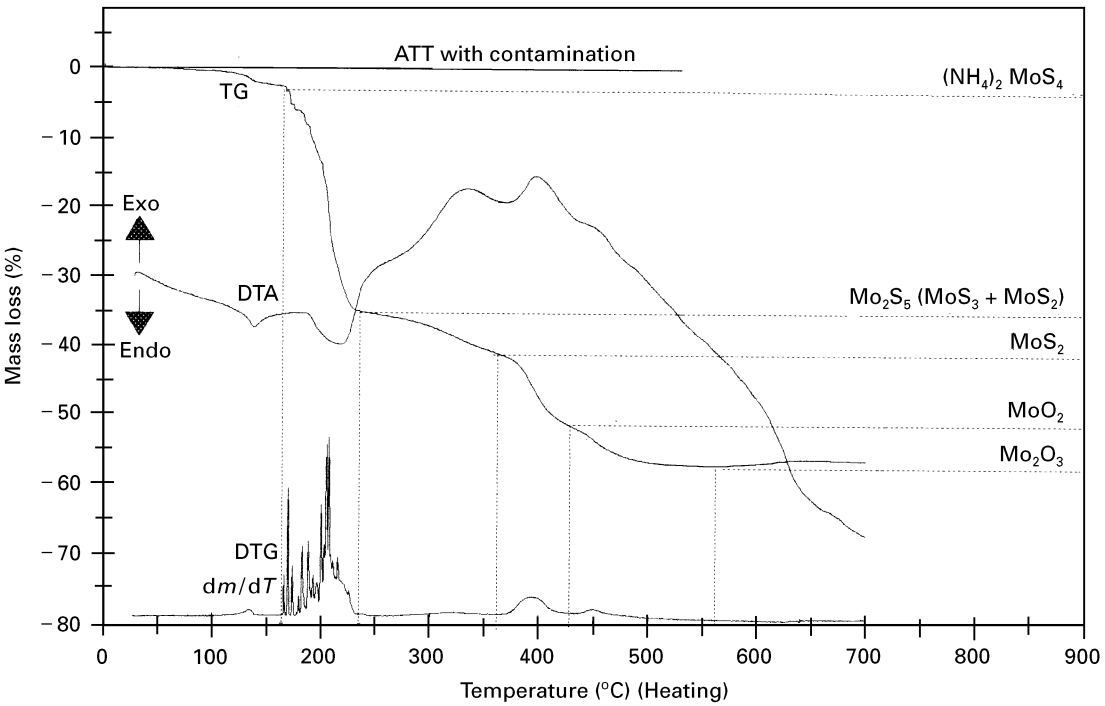

Figure 6 TG(ΔW-T), DTA(ΔT-T) and DTG(dm/dt) curves for the thermal decomposition of ammonium tetrathiomolybdate crystals. (ATT: ammonium tetrathiomolybdate).

MoS_2 by decomposition of MoS_3 were most probably superimposed or too close to be distinguished from each other. A slower temperature ramp (e.g. $2\,^{\circ}C\,min^{-1}$) is expected to provide more precise information on the transitions. Nevertheless, the present TGA/DTA studies, together with the XRD and SEM investigations, have confirmed the possibility of synthesis of 3R-MoS_2, from both MoS_3 and $(NH_4)_2MoS_4$ crystals, over a wide temperature range, and clarified the reaction mechanisms.

The findings of the study suggest that the sulphide generated during anodizing of aluminium in thiomolybdate electrolyte is probably amorphous MoS_3, possibly containing a small amount of crystalline MoS_2, which is trapped within the pores of porous anodic films. However, the amorphous product is relatively easily decomposed with moderate heating to form crystalline MoS_2. The necessary heating for formation of MoS_2 is unlikely during anodizing since temperature rises from Joule heating are estimated to be generally only a few tens of degrees [34] but may be achieved by frictional heating during wear, particularly at hot spots on the contacting surfaces, thus providing a possible explanation of the reported [17] improved tribological performance of anodized surfaces.

Acknowledgement

The authors wish to thank the Engineering and Physical Science Research Council for financial support. Special thanks are due to Mrs M. Tout and Professor F. R. Sale, Mr I. Brough, and Mr J. Birchall at the Manchester Materials Science Centre for their assistance in the TGA/DTA, XRD and vacuum heat treatment, respectively.

References

1. M. S. WHITTINGHAM, *Sci.* **192** (1976) 1126.
2. D. S. TAKUR and B. DELMON, *J. Catal.* **91** (1985) 308.
3. J. A. OGILVY, *Wear* **160** (1993) 171.
4. R. L. FUSARO, *American Society of Lubrication Engineers Trans.* **25** (1982) 141.
5. W. O. WINER, *Wear* **10** (1967) 422.
6. R. MURRAY and B. L. EVANS, *J. Appl. Cryst.* **12** (1979) 312.
7. R. N. VISWANATH and S. RAMASAMY, *J. Mater. Sci. Lett.* **25** (1990) 5029.
8. S. H. EL-MAHALAWY and B. L. EVANS, *J. Appl. Cryst.* **9** (1976) 403.
9. A. A. AL-HILLI and B. L. EVANS, *J. Cryst. Growth* **5** (1972) 93.
10. J. MERING and A. LEVIALDI, *C.R. Acad. Sci. Paris* **213** (1941) 798.
11. C. N. R. RAO and K. P. PISHARODY, *Prog. Solid State Chem.* **10** (1975) 207.
12. J. C. WILDERVANCK and F. JELLINEK, *Z. Anorg. Allgem. Chem.* **328** (1964) 309.
13. A. VAZQUEZ, J. M. DOMINGUEZ, C. PINA, A. JAIDAR and S. FUENTES, *J. Mater. Sci. Lett.* **9** (1990) 712.
14. B. C. STUPP, *Thin Solid Films* **84** (1981) 257.
15. S. CHANDRA and S. N. SAHU, *J. Phys. D.* **17** (1984) 2115.
16. P. PRAMANIK and S. BHATTACHARYA, *J. Mater. Sci. Lett.* **8** (1989) 781.
17. G. GUANG, Y. WU, J. LI and H. LIU, *Acta Metall. Sinica B* **6** (1993) 102.
18. K. ISAWA, M. MAEJIMA and K. SARAWATARI, *New Mater. New Process.* **2** (1983) 420.
19. A. W. BRACE and M. G. FAUL, *Trans. Inst. Met. Finish.* **66** (1988) 133.
20. R. G. DICKINSON and L. PAULING, *J. Amer. Chem. Soc.* **45** (1923) 1466.
21. Y. TAKEUCHI and W. NOWACKI, *Schweiz. Mineral. Petrogr. Mitt.* **44** (1964) 105.
22. F. E. WICKMAN and D. K. SMITH, *Amer. Mineral.* **55** (1970) 1843.
23. J. W. FRONDEL and F. E. WICKMAN, *ibid.* **55** (1970) 1857.
24. R. J. J. NEWBERRY, *ibid.* **64** (1979) 758.
25. *Idem*, *ibid.* **64** (1979) 768.
26. E. P. KHLYBOV, G. M. KUZ'MICHEVA and V. V. EVDOKIMOVA, *Russ. J. Inorg. Chem.* **31** (1986) 627.
27. R. CHEVREL, M. SERGENT and J. PRIGENT, *Mater. Res. Bull.* **9** (1974) 1487.
28. J. M. TARASCON and G. W. HULL, *ibid.* **21** (1986) 859.
29. F. MAWROW and M. NOKOLOW, *Z. Anorg. Allgem. Chem.* **95** (1916) 188.
30. ASTM Diffraction Data File, Card No. 17-744.
31. P. RATNASAMY, L. RODRIQUE and A. J. LEONARD, *J. Phys. Chem.* **77** (1973) 2242.
32. E. Y. RODE and B. A. LEBEDEV, *Russ. J. Inorg. Chem.* **6** (1961) 608.
33. W. W. WENDLANDT, "Thermal Methods of Analysis", 2nd Edn (John Wiley & Sons, New York, 1974) pp. 9–28.
34. F. R. APPLEWHITE, J. S. L. LEACH and P. NEUFELD, *Corros. Sci.* **9** (1969) 305.

Received 19 October
and accepted 20 November 1995